

## INPUT COUPLER FOR SUPERCONDUCTING ACCELERATOR STRUCTURE

A.A.Komkov, O.L.Maslennikov, V.F.Petrov, V.L.Smirnov, B.A.Sokolov

D.V.Efremov Scientific Research Institute of Electrophysical Apparatus, Leningrad, USSR

The design of a variable rf input coupler connected to the beam tube outside the endplate of the superconducting accelerator structure is discussed. Some considerations which define the choice of the coupler dimensions are given. The fine frequency tuning of the accelerator structure is performed through another tube branched off the beam tube. More than ten-year operational experience of the capture section for the superconducting electron linac is briefly reviewed.

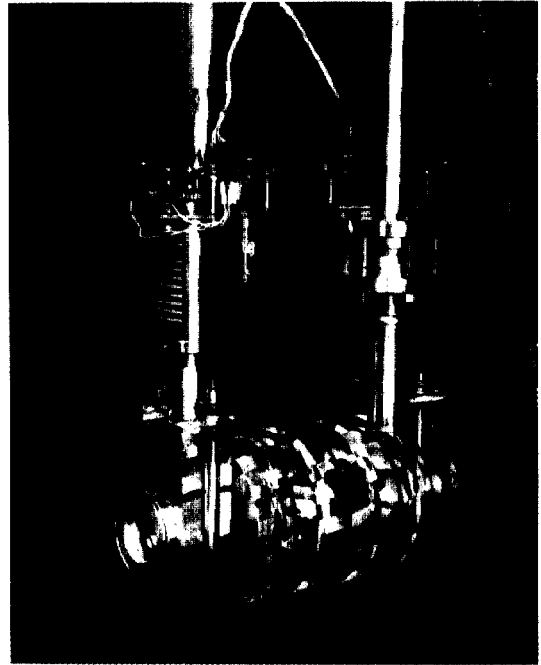
Operational parameters of the rf superconducting accelerating structures are determined by the state of the surface and purity of the superconductor used as well as by presence of the different system elements which may induce the local overvoltages. Such an element obligatory in this case is an rf input coupler. Insertion of the coupling element (hole, probe, loop) into the cavity volume produces some perturbation in the electromagnetic field which can induce quenching caused either by field emission or by thermal breakdown. Besides, additional losses may occur to give some reduction of  $Q_0$ -factor /1/.

For the first time, a method of rf excitation of the superconducting accelerator through a small hole drilled in the wall of the beam tube has been proposed for use in the capture section of our test superconducting linac ( $f = 2.8$  GHz). First electron beam tests of the capture section fitted up with such rf input assembly were made in 1976 /2/. Following operational experience has demonstrated good reliability of the capture section /3/. The rf input coupler is simple in fabrication and handling and does not introduce any additional rf losses or field disturbances. At present, the rf input assemblies of similar design are widely used /4/.

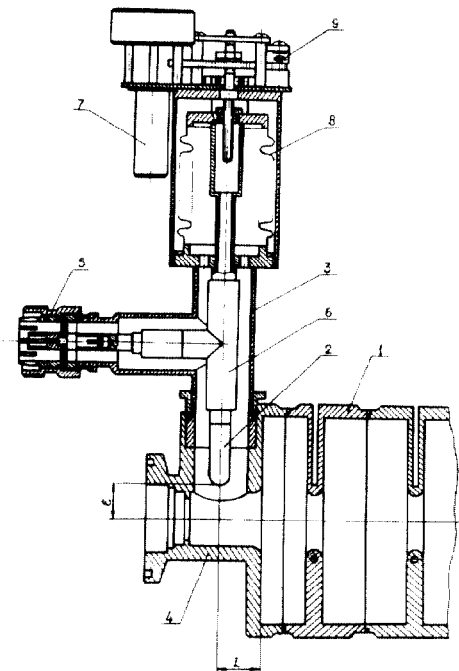
In our version of the rf input assembly the coupling hole is located at  $L = 17$  mm away from the inner wall of the cavity endplate (Fig.1). Knowing the  $L$  distance one can alternatively find either maximum value of the coupling coefficient,  $\beta_{max}$ , at a given  $Q_0$  or the smallest  $Q_0$  at  $\beta = 1$ . The coefficient can be varied by adjusting the probe position  $l$  inside a tube branched off from the beam tube at a right angle. The ratio  $\beta/Q_0$  is constant if the coupling is fixed. The dependence of  $\beta/Q_0$  upon  $l$  can be approximated by

$$\beta/Q_0 = Ae^{-2\alpha l}$$

where  $A$  is the factor determined by the coupling assembly design, and  $\alpha$  is the attenuation constant for cut-off tube containing the coupling element.



a



b

Fig.1. a) Capture section with rf coupling assembly, b) Schematic of rf coupling assembly, 1-capture section, 2-coupling element, 3-tube containing the coupling element, 4-beam tube, 5-connection to rf line, 6-fixed inner conductor of coaxial line, 7-motor drive, 8-bellows, 9-probe position indicator

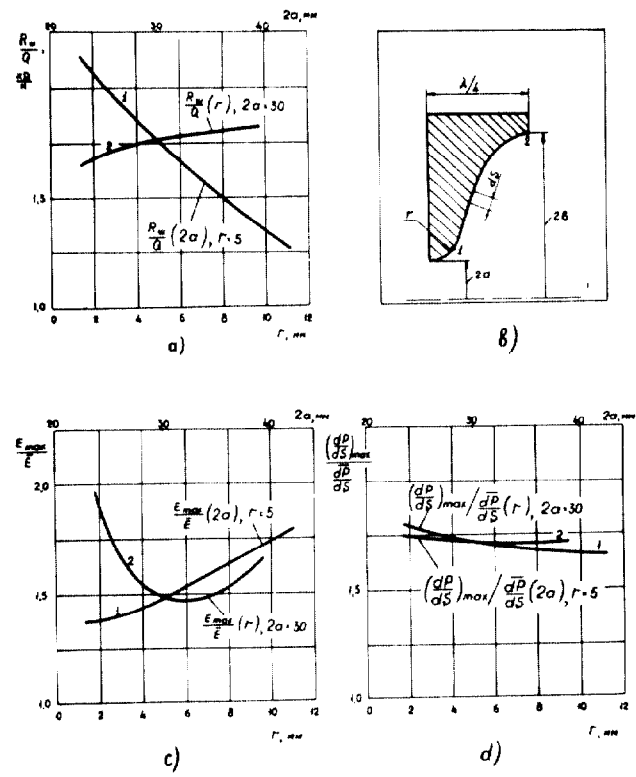
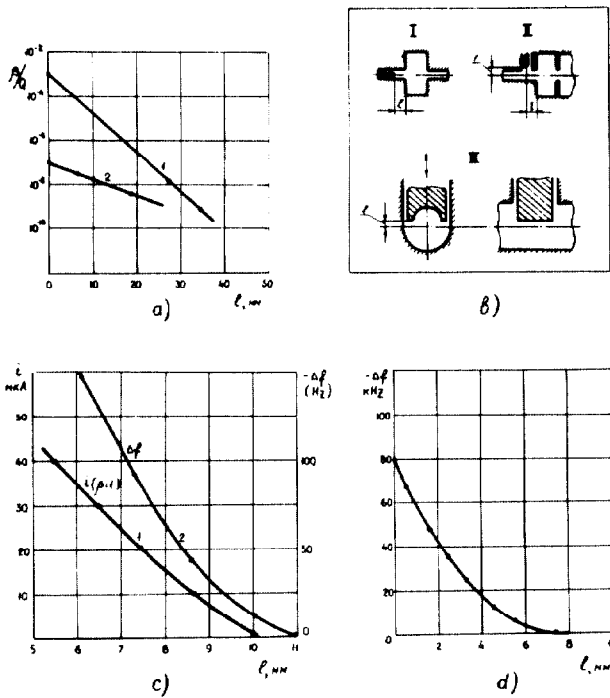


Fig.2. Experimental data:  
 a)  $\beta/Q_0$  ratio for a one cell  $E_{01}$ -cavity (curve 1) and for a four cell  $\pi$ -mode capture section (curve 2) versus coupling element location  $l$ .  
 b) schematic view of the coupling element location in a one cell  $E_{01}$ -cavity (I), in a capture section (II) and the location of the frequency tuning element in the capture section beam tube (III)  
 c) curve 1 - beam current versus probe location  $l$  in the rf coupling assembly of the capture section under matching conditions ( $\beta=1$ ); curve 2 - variation of the capture section frequency shift at zero beam current ( $f=2.8$  GHz,  $Q_0=6 \cdot 10^7$ ,  $4.2^\circ\text{K}$ ) versus  $l$ ;  
 d) variation of the capture section frequency shift versus the tuning plunger location  $l$  in the tube branched off from the beam tube at a right angle (see Fig.2b, III)

Fig.3. Calculated data for the  $\pi$ -mode structure with the cell profile shown in Fig.3b and with normalized phase velocity equal to unity at  $f=2.8$  GHz:  
 a)  $R/Q$  ratio;  
 b) the ratio of the maximum electric field,  $E_{max}$ , on the cell surface (taken at point 1, Fig.3b) to the field averaged over the structure axis;  
 d) the ratio of the maximum rf losses per unit square (taken at point 2, Fig.3b) to rf losses averaged over the entire cell surface.  
 Curves 1 in Figs.3a,3c,3d represent the dependences of the above said quantities with the aperture diameter,  $2a$ , at fixed edge radius  $r = 0.5$  cm;  
 Curves 2 show those dependences with respect to the edge radius at  $2a = 3.0$  cm ( $a/\lambda = 0.14$ )

Fig.2a demonstrates experimental curves for two set-ups:  
 1. The welded, one cell  $E_{01}$ -cavity machined out from Nb casting. The probe is movable along the beam tube;  $A=10^{-3}$ ;  $\alpha=2.2$  cm $^{-1}$ .  
 2. The 4 cell niobium capture section. The probe is movable along the tube, branched off from the beam tube;  $A=10^{-7}$ ;  $\alpha=0.86$  cm $^{-1}$ .  
 Another dependence which appears to be of considerable interest is the variation of coupling coefficient with the beam current. Curve 1, plotted in Fig.2c, illustrates the variation of the probe location  $l$  versus beam current measured under matching conditions ( $\beta=1$ ). Curve 2 shows the variation of the resonant frequency shift,  $\Delta f$ , with  $l$  for the capture section. It is seen that a very accurate tuning of the resonant frequency can be obtained with such a probe.

The tuning range can be essentially broadened, if the plunger with profile shown in Fig.2b is employed instead of the probe. The frequency tuning in the range of 80 kHz has been obtained (Fig.2d) while the relevant nonuniformity of the axial field distribution was observed to be within 2%. This tuning procedure can be also employed to correct the fabrication frequency errors of the individual sections which constitute the multi-section linac.

Certainly, the frequency tuning range of the section is determined by a total number of cells  $N$  and, for example, is doubled when  $N$  is halved. However, the tuning range can be noticeably expanded by increasing the beam tube diameter, i.e. by decreasing the relevant attenuation constant. For fabrication simplicity, the beam tube diameter is usually

taken equal to the aperture diameter  $2a$  in the disk loaded waveguide. We chose  $2a=30$  mm ( $a/\lambda = 0.14$ ) for the 9 cell  $\pi$ -mode accelerating cavity being manufactured from the sheet niobium with residual resistance ratio  $RRR=300$ . The curves of Fig.3 represent the calculated values of the  $R/Q$  ratio, the peak to average electric field strength responsible for field emission and the peak to average rf losses per unit square versus  $2a$ . The curves showing the variation of these quantities versus the edge radius of the disk aperture are also plotted in Fig.3. It is noteworthy that all of these characteristics vary rather smoothly over the wide range of  $r$  thus giving the preference to the manufacture considerations while the cell profile is being chosen. The data represented in Fig.3 were computed with the "PRUD-0" code /5/.

#### LITERATURE

1. Bauer W. et al. Design Study of a Superconducting Deflected Cavity. IEEE Trans. Nucl.Sci., 1971, NS-18, p.181.
2. Vakhrushin Yu.P. et al. Start-up of Superconducting Accelerator. Problems on Atomic Science and Engineering. Series: Linear accelerators, issue (4), Khar'kov, KhPTI, 1977, p.5.
3. Vakhrushin Yu.P. et al. Study of Superconducting Corrugated Waveguide. Proceedings of VII All-Union Meeting on Charged Particle Accelerators. V II. Dubna. JINR, 1981, p.40.
4. Benvenuti G. et al. RF-Superconductivity at CERN-Proceedings of the Second Workshop on RF-Superconductivity, P.1. CERN, Geneva, 1984, p.25-48.
5. Abramov A.G. et al. PRUD-0 Program Package to calculate accelerating structures. Preprint IPHE 83-3, Serpukhov, 1983.